

UNCLASSIFIED

AD NUMBER
AD845078
NEW LIMITATION CHANGE
TO Approved for public release, distribution unlimited
FROM Distribution authorized to U.S. Gov't. agencies and their contractors; Administrative/Operational Use; DEC 1968. Other requests shall be referred to Army Missile Command, Redstone Arsenal, AL.
AUTHORITY
USAMC ltr, 23 Aug 1971

THIS PAGE IS UNCLASSIFIED

8205078

COPY

638

A. D.

Technical Report 8-152

DEVELOPMENT OF A BALL INDENTATION TEST  
FOR SAMPLES OF FINITE THICKNESS

by

William M. Sigmon  
Charles H. Parr  
Albert J. Ignatowski

December 1968

U. S. ARMY MISSILE COMMAND  
REDSTONE ARSENAL, ALABAMA 35803

Contracts

DAAH01-67-C-0655

DAAH01-68-C-0632

ROHM AND HAAS COMPANY  
REDSTONE RESEARCH LABORATORIES  
HUNTSVILLE, ALABAMA 35807

DDC  
DEC 2 1968

### DISTRIBUTION LIMITATION

Initial distribution of this report has been made in accordance with contractual agreements and approved supplements received from our Contracting Officer. Qualified government agencies and contractors may obtain this report from the Defense Documentation Center, Cameron Station, Building 3, Alexandria, Virginia 22304.

This document is subject to special export controls, and each transmittal to foreign governments or foreign nationals may be made only with prior approval of:

SEARCHED BY		
DATE	WRITE MEMO <input type="checkbox"/>	
CS	REF SERVICE <input checked="" type="checkbox"/>	
UNCLASSIFIED	<input type="checkbox"/>	
RESTRICTION		
BY		
DISTRIBUTION/AVAILABILITY CODES		
DIST.	AVAIL.	SPECIAL
2		

Department of Army  
Headquarters, U. S. Army Missile Command  
Redstone Arsenal, Alabama 35899

### DISCLAIMER

The findings in this report are not to be construed as an official Department of the Army position unless so designated by other authorized documents.

### DISPOSITION INSTRUCTIONS

Destroy this report when no longer needed. Do not return it to the originator.

December 1968

Technical Report S-182

**DEVELOPMENT OF A BALL INDENTATION TEST  
FOR SAMPLES OF FINITE THICKNESS**

by

**William M. Sigmon  
Charles H. Parr  
Albert J. Ignatowski**

STATEMENT #2 UNCLASSIFIED

This document is subject to special export controls and each transmittal to foreign governments or foreign nationals may be made only with prior approval of

**U. S. ARMY MISSILE COMMAND  
Redstone Arsenal, Alabama 35809**

*Att: AMSM1-RK*

Contracts  
DAAH01-67-C-0655  
DAAH01-68-C-0632

Distribution Limited

**ROHM AND HAAS COMPANY**

**REDSTONE RESEARCH LABORATORIES**

HUNTSVILLE, ALABAMA 35807

## FOREWORD

The work described in this report was performed under Contracts DAAH01-67-C-0655 and DAAH01-68-C-0632 for exploratory development of propellants for missiles and rockets under the technical cognizance of the Solid Propellant Chemistry Branch, Army Propulsion Laboratory and Center, Research and Development Directorate, U. S. Army Missile Command.

The propellant chemist often requests the mechanical testing laboratory to supply some form of quantitative laboratory measure of the mechanical behavior of small quantities of low modulus propellant binder gumstocks. Frequently these materials are ill-suited for the usual gamut of mechanical property tests developed for finished propellants. Mechanical property data supplied at an early phase of propellant binder development can be useful in determining proper curing systems and conditions, effects of plasticizers or other modifiers, effects of variations of binder synthesis or processing, and can give indications of glass transition temperature, strain rate dependency, and other factors which are important in the finished propellant. The test developed here is useful in these applications and deviates from previous hardness, indentation, or flexure tests in that the accompanying data analysis includes the effect of finite sample dimensions.

The work described here grew out of work first initiated under Contract DA-01-021 AMC-11536(Z).

## ABSTRACT

A spherical indentation test for small quantities of low modulus materials is described and experimentally validated. The data analysis takes into account finite sample thickness. Comparison with the Hertz contact theory is made, and extension to viscoelastic characterization is discussed.

## CONTENTS

	<u>Page</u>
Foreword	iii
Abstract	iv
Section I. INTRODUCTION	1
Section II. ANALYSIS OF THE INDENTATION TEST	3
1. Elastic Materials	3
2. Viscoelastic Materials	7
Section III. DESCRIPTION OF EXPERIMENTAL EQUIPMENT AND PROCEDURES	10
1. Test Device	10
2. Test Procedures	10
Section IV. EXPERIMENTAL RESULTS AND DISCUSSION	14
1. Evaluation of Test Device and Method	14
2. Viscoelastic Materials Test	18
Section V. CONCLUSIONS	23
References	25
Appendix SOLUTION OF THE INDENTATION PROBLEM	27
1. The Lebedev-Ufliand Solution	27
2. Application to the Indentation Test	33
3. Numerical Solution of Equations	35

## Section I. INTRODUCTION

A ball indentation test has been developed to meet the need for a simple, practical method of measuring the shear modulus of laboratory quantities of rubbery materials. The indentation test offers a number of possible advantages: sample size and shape are noncritical and only a minimum of preparation is needed; the quantities of sample material required are relatively small; the test device is simple and easy to operate; the method is non-destructive in character, thus permitting repeated tests on the same sample.

Many of the previous applications of the indentation test were limited by lack of a well-defined relationship among applied load, indenter geometry, indentation depth, and the material shear modulus, particularly for thin test samples. Most work in the past made use of either the classical Hertz contact theory or of some modification of it based upon empirical test data [1-4]. The Hertz solution, discussed in many texts on elasticity (e. g., Timoshenko and Goodier [5]), assumes the indented solid to be a semi-infinite layer, i. e., of infinite depth below the deformed surface. Therefore, in the design of a practical test, questions arise as to (1) the limits of finite specimen size and indentation for which the Hertz theory will apply with sufficient accuracy, and (2) other relationships which may be used for those cases where the Hertz theory will not provide results of the required accuracy.

Hitherto, mainly because no precise information was available, the classical theory was assumed to hold for an indentation not exceeding 10 percent of the specimen thickness [1, 2, 4]. Gent [2], for example, has shown that the Hertz theory is quite accurate for determining Young's modulus of vulcanized rubbers when using small indentations, up to one-tenth the sample thickness. Waters [4] conducted a series of tests, using spherical indentors on sheets of vulcanized rubber of various thicknesses, and found that moduli computed by the Hertz theory were in error by less than 5 percent when the sheet thickness was more than 8 times the indenter contact area radius. With thinner sheets, much larger errors were experienced, exceeding 30 percent for thicknesses less than 4 times the contact radius. Waters' approach to the problem was to modify the Hertz expression by an experimentally derived function involving the ratio of thickness to contact area and including a constant to allow for the surface conditions (lubricated and dry).

None of these methods are particularly applicable to the problem of measuring the shear modulus of "soft" polymers (those

with moduli less than  $10^3$  psi) in the form of relatively thin sheets. In order to have indentation depths and forces sufficiently large to be recorded accurately by conventional instruments, the specimen must be indented to a considerable fraction of its total thickness, therefore deviating markedly from the Hertz model. Empirical formulas are of doubtful value, considering the wide range of materials encountered. However, Lebedev and Ufliand [6] have dealt with the problem of pressing a rigid axisymmetric punch of any profile into an elastic layer of finite thickness. Their solution offers the possibility of obtaining a firm theoretical relationship among load, indentation, and shear modulus for tests of rubbery materials in readily available forms. Parr [7, 8] has applied the Lebedev-Ufliand solution to the specialized case of a spherical indenter, with particular emphasis on obtaining a relationship in a form most useful to the test laboratory. The results of this analysis led to the development of the ball indentation test method described herein.

## Section II. ANALYSIS OF THE INDENTATION TEST

### 1. Elastic Materials

The ball indentation test may be considered as a special case of the general problem of a punch penetrating a solid. The geometry is shown in Figure 1. The object of the analysis is to find a solution relating the unknown shear modulus of the test sample to the known or measurable quantities of indenter radius  $R$ , applied load  $P$ , and penetration  $w_0$ , for any thickness,  $h$ , of sample material. The materials to be tested by this method will have elastic moduli several orders of magnitude smaller than those of steel or aluminum, of which the test device is constructed; therefore, for practical purposes the indenter and base may be considered infinitely rigid.

The solution to the problem is outlined in the Appendix. Briefly stated, the solution consists of using the method developed by Lebedev and Ufliand to express displacements and stresses in terms of one auxiliary function, which represents the solution of a Fredholm integral equation. The general solution is reduced to the specific case of a spherical indenter, and equations are obtained for applied load and indenter penetration in terms of the auxiliary function. The expressions thus obtained are too complex to be evaluated exactly, therefore, numerical methods are employed to compute values of the auxiliary function. These values, in turn, are used to solve for load and penetration by quadrature.

The results are presented in Figures 2 and 3. These sets of curves are taken from the paper of Ignatowski and Parr [8] in which the analysis originally appeared. In Figure 2 the dimensionless load  $(1-\nu)P/\mu R^2$  is plotted versus dimensionless indentation  $w_0/R$  for various values of the dimensionless thickness ratio  $h/R$  ( $\nu$  is Poisson's ratio and  $\mu$  the shear modulus). Figure 3 presents the same information in a different manner, with indentation as the abscissa and curves for various values of thickness ratio. Note that the elastic constants of the material appear only in the dimensionless load; all computations are independent of the elastic constants. This situation results from the boundary conditions imposed, in which frictionless contact between the test sample and base or indenter is assumed.

Dimensionless quantities were chosen for the calculations and Figures 2 and 3 for the sake of convenience and generality, but these quantities may not necessarily be the most convenient for actual test data reduction. The curves can easily be modified to apply to any particular laboratory setup. With the indenter radius

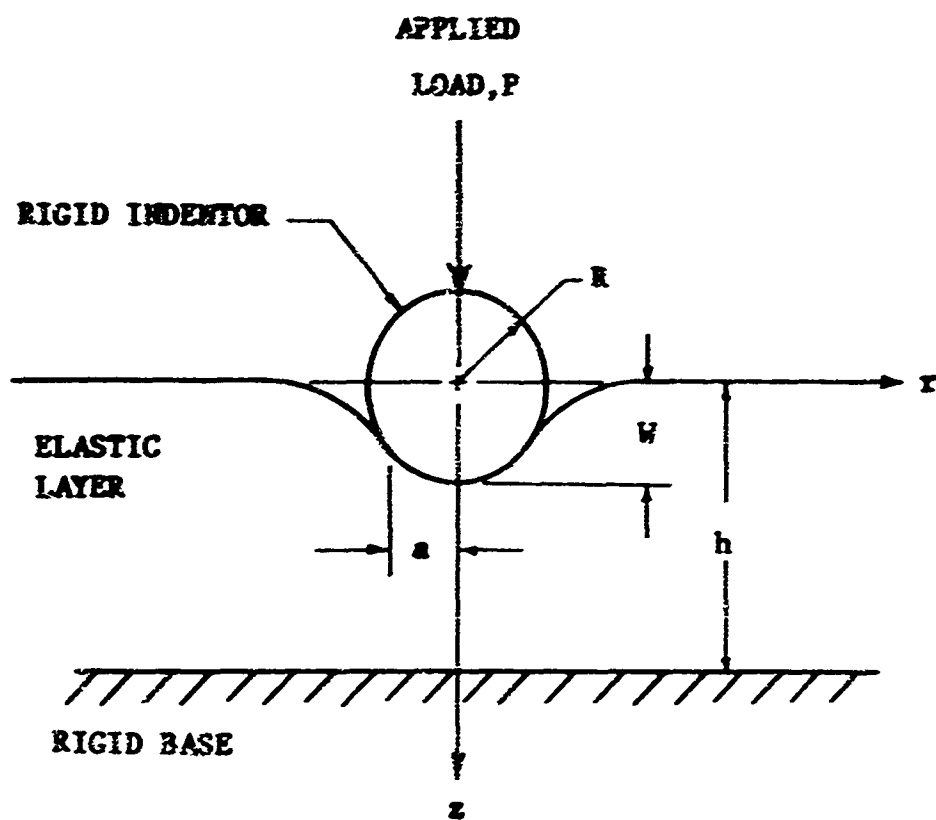


FIGURE 1. GEOMETRY OF INDENTATION PROBLEM

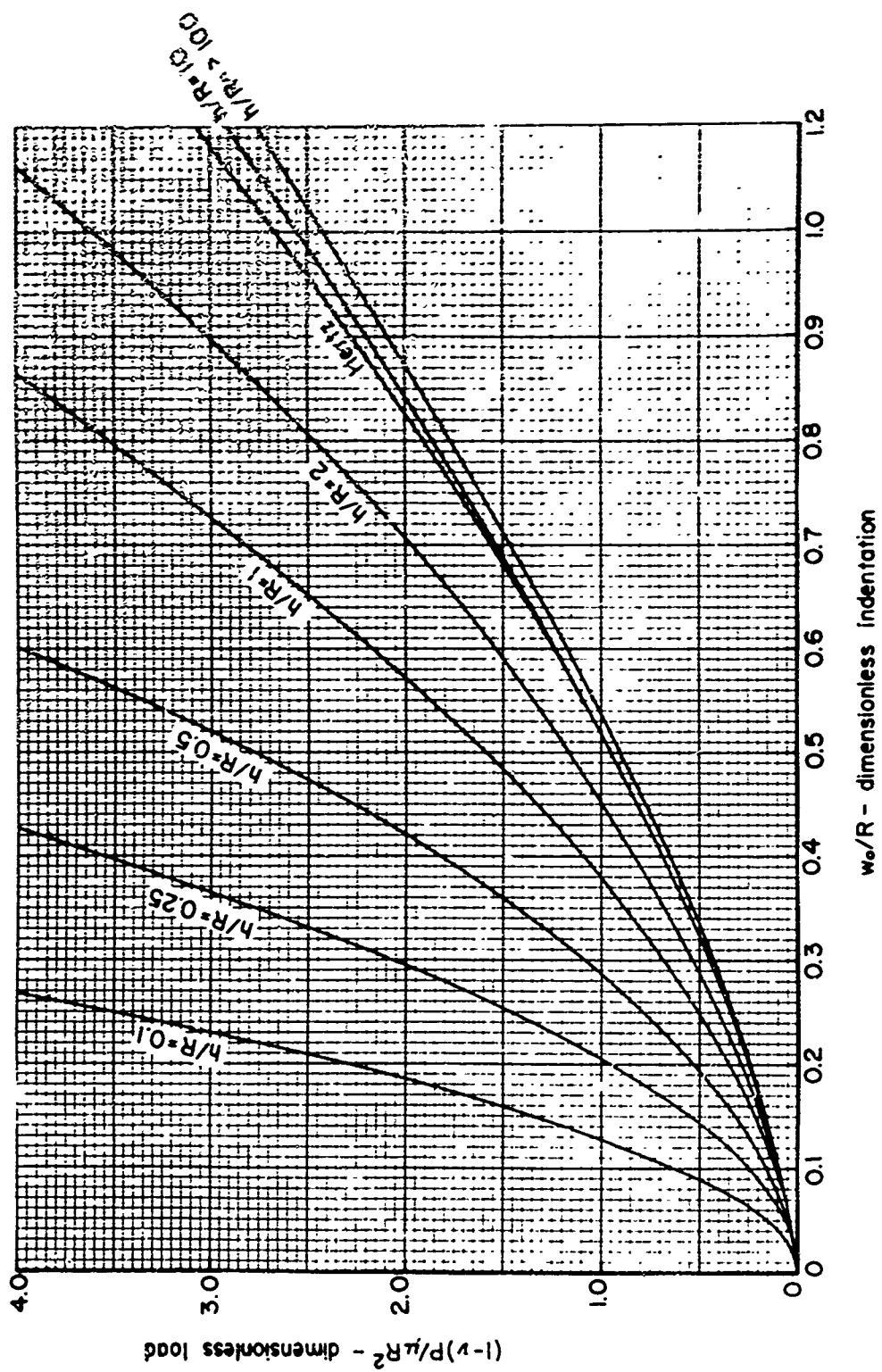


FIGURE 2. DIMENSIONLESS LOAD VS. DIMENSIONLESS INDENTATION FOR VARIOUS DIMENSIONLESS THICKNESS VALUES

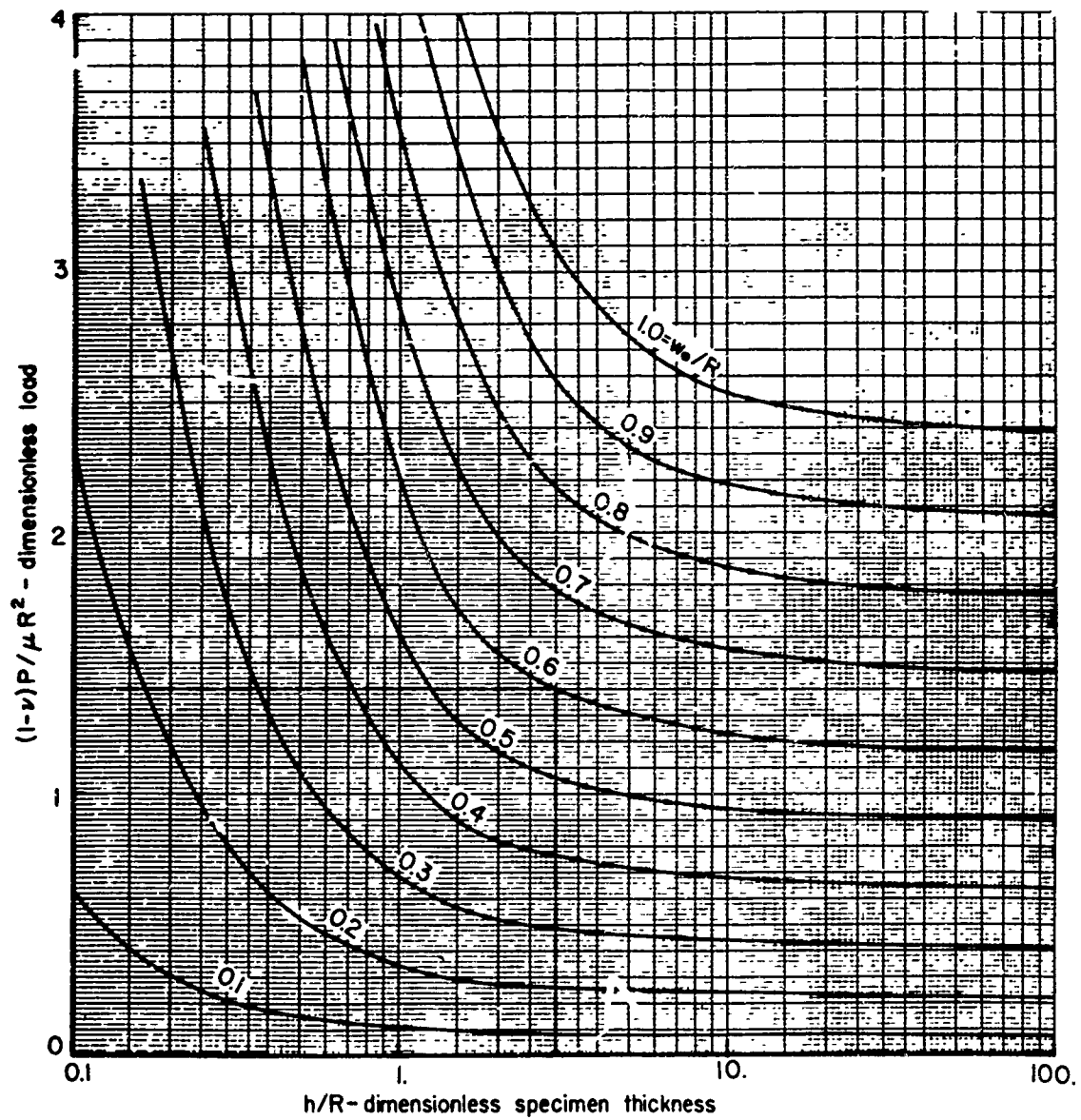


FIGURE 3. DIMENSIONLESS LOAD VS. DIMENSIONLESS THICKNESS FOR VARIOUS DIMENSIONLESS INDENTATION VALUES

known, and Poisson's ratio known or assumed ( $\nu = 0.5$  is a very good approximation for rubbery materials), curves of  $P/\mu$  versus  $w_0$  for various values of  $h$  (from Figure 2), or versus  $h$  for various values of  $w_0$  (from Figure 3), are obtained. The shear modulus can then be determined from laboratory measurements of  $P$ ,  $h$ , and  $w_0$ . A different set of curves is required for each indenter radius and Poisson's ratio, but these are available simply by changing the scales on the basic curves in Figures 2 and 3.

The curve of the classical Hertz contact problem solution is included in Figure 2 for comparison with the Lebedev-Ufliand solution. Note that the two essentially agree for specimen thicknesses in excess of ten indenter radii. However, for thinner specimens, drastic differences between the solutions are seen. The Hertz theory, developed for a semi-infinite layer, does not consider the effects of finite thickness which become prominent for relatively thin layers. For example, for a specimen thickness of one indenter radius ( $h/R = 1$ ) the Hertz theory gives a shear modulus value some 35 percent higher than that given by the Lebedev-Ufliand curves. Additional comparisons will further define the practical limits of the classical theory and illustrate the hazards of its misuse with thin sections.

## 2. Viscoelastic Materials

Strictly speaking, the foregoing discussion and the analysis given in the Appendix pertain only to elastic materials. However, since many, perhaps most, materials of interest exhibit viscoelastic behavior, it becomes important to know how the indentation test may be applied in measurement of viscoelastic properties.

Through the processes of stress relaxation, certain viscoelastic materials, subjected to a constant strain, will eventually reach a condition of equilibrium for which the stress remains constant with time. Moduli corresponding to this condition are known as equilibrium, long-time, or "rubbery" moduli, and may be computed from indentation test data and the results of the elastic analysis, just as with an elastic material. In other words, the material is assumed to have reached a state where the shear modulus is independent of time as it is in an elastic material. The only requirement is to wait a sufficient length of time before taking readings to insure that equilibrium has been reached.

For shorter ranges of time when equilibrium stress-strain conditions have not been achieved, or for tests where the purpose is

measurement of short-time effects such as relaxation moduli, the indentation test and its elastic solution also appear useful. However, the problem of application becomes considerably more difficult.

The information in Figure 2 may be considered as described by

$$\frac{P}{\mu} = f(w_0) \quad (1)$$

where  $f(w_0)$  is a function known only graphically. Lee and Radok [9] have shown that the viscoelastic counterpart of the Hertz contact theory can be deduced from the elastic solution. By analogy, we may say that

$$P(t) = \int_0^t \mu(t-\tau) \frac{df(w_0)}{d\tau} d\tau \quad (2)$$

where  $\mu(t)$  is the shear relaxation modulus, and  $f(w_0)$  is time dependent because  $w_0$  is time dependent. Equation (2) may be solved for  $\mu(t)$  if the time dependency of  $f(w_0)$  is known. This, however, is not easily done even if  $w_0(t)$  is known because  $f(w_0)$  is a complex function of  $w_0(t)$ .

One useful case, for which there is a relatively simple solution, is that of a step function input. If  $w_0(t)$  is applied as a step function, or instantaneous, penetration, then  $f(w_0)$  is also a step function and (2) reduces to

$$P(t) = \mu(t) f(w_0) \quad (3)$$

The dimensionless load in Figure 2 can then be interpreted as

$$\frac{(1-\nu)P(t)}{R^2\mu(t)}$$

Knowledge of the load-time history,  $P(t)$ , permits calculation of the shear relaxation modulus  $\mu(t)$ .

In actual practice a step function is, of course, not achieved. Some finite time,  $t_1$ , is required for the indenter to reach the desired penetration depth. Nevertheless, for many materials it may be possible, with suitable high-speed test devices, to reduce  $t_1$  to

values much less than the times of interest and thus be able to consider  $w_0(t)$  a step function for all practical purposes. Following the same approximation often used in tensile stress relaxation testing [10], it appears reasonable to assume a step function input for times greater than  $10 t_1$ .

### Section III. DESCRIPTION OF EXPERIMENTAL EQUIPMENT AND PROCEDURES

#### 1. Test Device

A simple prototype test device was initially built to obtain an approximate comparison between the theoretical analysis and experimental data. The results were encouraging, and so a more refined design model was constructed according to the sketch of Figure 4. The ball indentation test device shown in Figure 4 somewhat resembles two interleaved C-clamps. The upper "C" supports the test specimen and is designed to be suspended from a load cell by means of a pull rod with universal joints. It is counterweighted and balanced so as to hang freely with the pull rod centerline vertical. The spherical indenter is mounted in the lower "C," which is attached by another pull rod to the movable crosshead of a universal tensile testing machine. With the test specimen and indenter located between the overlapping arms of the "C"s, the indenter is pressed into the specimen when the lower "C" is given a downward displacement. Scribe marks along the centerline of both parts facilitate alignment during assembly and operation.

The test device was originally designed to be used with Instron universal test machines, but is easily adaptable to many other loading arrangements. For example, a fixed support and a dead weight produce a creep tester. The small size of the device (approximately  $5 \times 3 \times 2$  inches overall, not including pull rods) enables it to be used in most available temperature and environmental chambers.

The indentors are commercially available, ground and polished, tungsten carbide balls, cemented to insert pins. The indentors are readily interchanged and are presently used in a range of sizes. Table I gives the sizes which are available. Maximum test specimen dimensions are 1.5 inches square by 0.75 inch thick. The test specimen base has been coated with Teflon<sup>®1</sup> to reduce friction.

#### 2. Test Procedures

The only test specimen preparation usually required is to cut the specimen to a size which will fit the test device. Very rough cuts are acceptable for the edges, with no restrictions on squareness. The contact surfaces, between the specimen and the base and indenter,

---

<sup>1</sup>Trademark of E. I. DuPont and Company, Wilmington, Del.

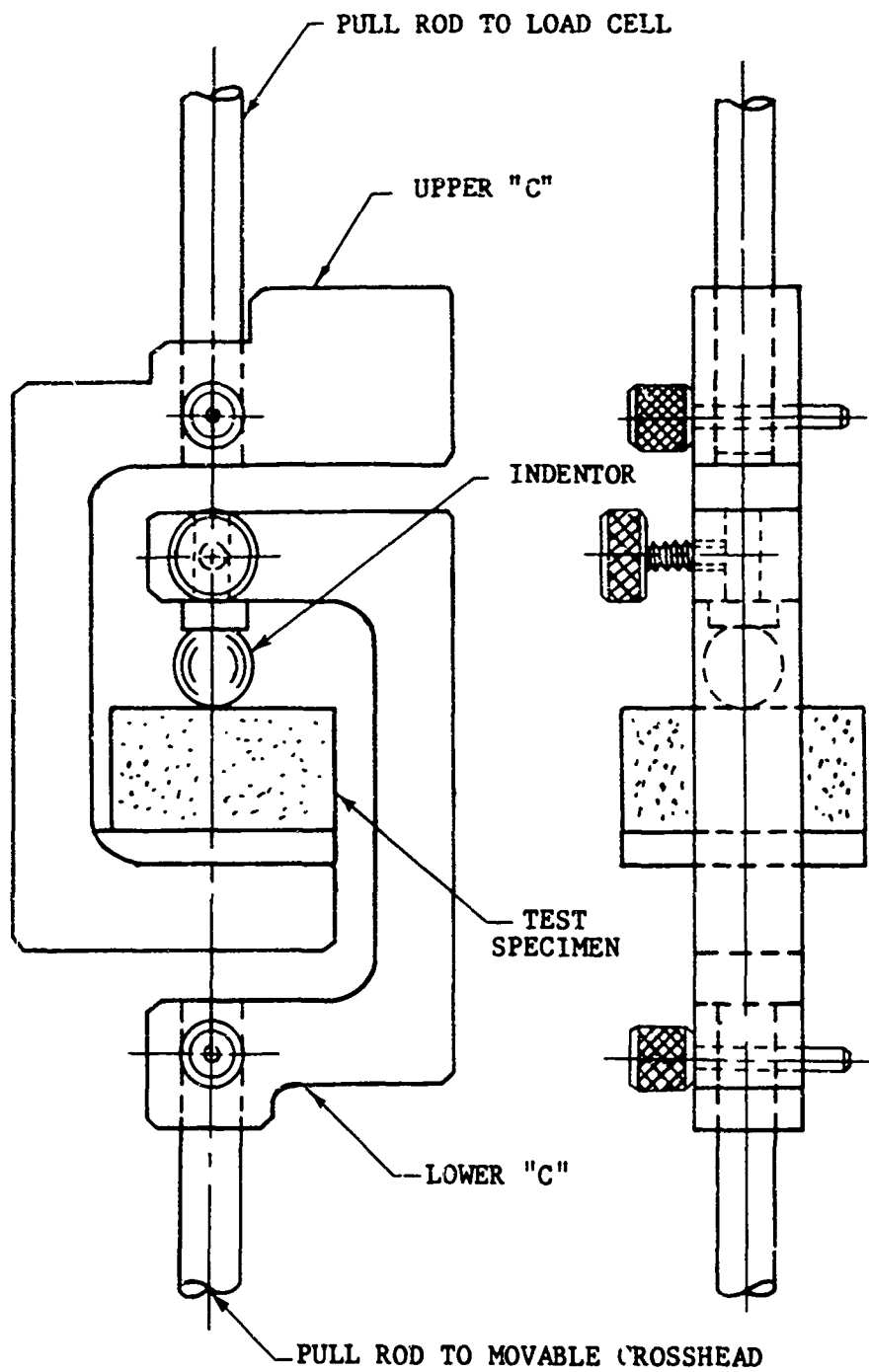


FIGURE 4. ASSEMBLY DRAWING, BALL INDENTATION TEST DEVICE

Table I. Indentation Test Data for Hysol 8705 Specimen

For all test conditions:

Specimen dimension approx. 1.5 in. sq.

Specimen thickness = h = 0.504 in.

Poisson's ratio =  $\nu$  = 0.46 from Mfg's specs

Penetration rate = 2.0 in./min

Temperature 77°F

Load readings taken after 2 min relaxation at constant indentation

Specimen surfaces dusted with talcum powder

Indenter Radius, R (in.)	h/R	Indentation Depth, $w_0$ (in.)	$w_0/R$	$\frac{(1-\nu)P}{\mu R^2}$ (Note 1)	Load, P (Note 2) (lb)	Computed Shear Modulus, $\mu$ (psi)
0.0625	8.05	0.025	0.40	0.69	1.05	212
		0.038	0.60	1.25	1.92	212
		0.050	0.80	1.92	2.97	214
0.0938	5.37	0.038	0.40	0.71	2.73	235
		0.056	0.60	1.30	4.74	222
		0.075	0.80	1.97	7.45	231
		0.094	1.00	2.72	9.92	223
0.1250	4.02	0.050	0.40	0.74	4.78	224
		0.075	0.60	1.34	8.80	227
0.1562	3.22	0.031	0.20	0.26	2.45	208
		0.062	0.40	0.76	7.19	209
0.1875	2.69	0.038	0.20	0.26	3.56	206
0.2188	2.30	0.044	0.20	0.27	5.70	234
0.2500	2.01	0.050	0.20	0.28	7.28	224
Mean Value =						220
Standard Deviation =						10
Note 1 - Dimensionless load values from curves, Figure 3.						
Note 2 - Average reading from 2 runs.						

should be reasonably flat, smooth, and parallel. Allowable deviations depend upon the particular test circumstances regarding desired accuracy, ease of operations, and specimen properties. Care must be taken about non-parallelism, however, because non-parallel surfaces will introduce horizontal force components which may cause appreciable errors, and, in extreme cases, even cause the indenter to slide across the specimen surface.

It is also suggested that the specimen surfaces be dusted with talcum powder or lubricated in some other fashion. The effects of surface conditions have not yet been investigated fully, but preliminary checks indicate more consistent results with lubricated surfaces. However, the possibility of contamination of the test sample must be considered in the choice of a lubricant, and if any doubts exist lubrication should be omitted entirely. The effect upon the test results would probably be minor.

Other limitations exist regarding the minimum test specimen dimensions. In the theoretical analysis the specimen was assumed to be infinite in extent, though of finite thickness. No analysis has yet been performed for a specimen of finite dimensions, but test results have yielded some useful guidelines. Apparently specimen dimensions are not at all critical so long as the length and width are at least 1.5 times the thickness and 6 times the radius of the largest indenter to be used. Reasons for choosing these values will be discussed in a later section.

The test procedure consists of displacing the lower "C" fixture and recording the applied load and indentation depth as functions of time. Indentation depths may be determined from the test machine indicator dials, a separate displacement transducer, or by reading elapsed time from the load-time record and multiplying by cross-head speed (if known and constant).

The fractional or percentage error in determining indentation depth may be minimized by going to as great a depth as possible, subject to the limitations imposed by specimen thickness and allowable loads. Penetration must not exceed the spherical radius, because the equation used for the contact surface contour in the analysis would then no longer apply. Smaller indenter sizes result in lower loads at a given indentation, but are limited in penetration depth; therefore, some compromise may be necessary.

## Section IV. EXPERIMENTAL RESULTS AND DISCUSSION

### 1. Evaluation of Test Device and Method

A number of different materials have been tested with the ball indentation test device, but the results of only a few will be presented herein for the purpose of illustration. Two test series of interest are those of Hysol<sup>2</sup> and Solithane<sup>3</sup> 113 polyurethane rubbers. These materials were used to evaluate the test device and method because their properties were well known from manufacturer's data or other test results.<sup>4</sup> Comparison of the shear moduli obtained from the indentation test with those obtained by other means provided a check on the validity of the analysis and the curves in Figures 2 and 3.

Specimens of both materials were tested in the same manner. The indenter was pressed at a constant rate into the specimen to a predetermined depth, and held constant at this depth for two minutes. The curves of Figure 3 were entered with the values of  $w_0$ ,  $R$ , and  $h$  used, along with the load,  $P$ , read after two minutes, and values of the shear modulus were obtained. This modulus was considered the equilibrium shear modulus,  $\mu_e$ , since an essentially constant value of load was reached well within the two minute waiting period.

Data from tests on the Hysol 8705 specimen are summarized in Table I. Note that the same specimen was tested with a number of different size indentors and various indentation depths. No significant differences in results were found for any of the different indentors or depths. This was an expected result, for there is no indication in the analysis that the test setup parameters should affect the computed shear moduli. The mean value of shear modulus and its standard deviation, calculated from the test data, are given in Table I as 220 psi and 10 psi, respectively. A shear modulus was also computed from Young's modulus and Poisson's ratio according to the familiar equation

---

<sup>2</sup>Trademark of Hysol Corporation, Olean, N. Y.

<sup>3</sup>Trademark of Thiokol Chemical Corp., Trenton, N. J.

<sup>4</sup>The specific Solithane sample tested was provided through the courtesy of Professor W. G. Knauss, and was one of the materials thoroughly characterized as part of the development of a standard crosslinked polymer program conducted at the California Institute of Technology under U. S. Air Force sponsorship.

$$\mu = \frac{E}{2(1 + \nu)} \quad (4)$$

where Young's modulus,  $E$ , was obtained by conventional tensile tests on specimens cut from the same sheet. The tensile test data gave an average  $E = 550$  psi, which in turn gives  $\mu = 190$  psi. Agreement between the two values of shear modulus is considered reasonably good.

Data from tests of the Solithane 113 specimen are presented in Table II. Again, a number of various size indentors and indentation depths were used, along with different penetration rates. As before, no significant differences were noted in the values of shear modulus found for any of the different test conditions. The shear modulus mean value and standard deviation were calculated to be 197 psi and 16 psi, respectively. The California Institute of Technology Materials Science group reported a value of 185 psi for the shear modulus of the particular sample tested, obtained by a torsional pendulum method. This is in good agreement with the indentation test results. Unfortunately, the amount of material available was not sufficient for tensile testing; therefore, no comparison could be made as was done with the Hysol specimens.

A brief investigation was made into the effect of surface lubrication which was of interest because the theoretical analysis assumed frictionless contact. The results are given in Table III. Although the quantity of data is rather meager, there definitely does appear to be a trend toward lower values of shear modulus with lubricated surfaces. The data also indicate a much greater difference with the wet soap solution than with the dry lubricant of talcum powder used for the test reported in Tables I and II, at least for these two particular materials. The need for additional investigation of surface conditions effects is clearly indicated. However, surface lubrication may be inadvisable with many materials of interest because of the possibility of the material absorbing or reacting with the lubricants and thus undergoing a change in properties.

When the amount of indentation becomes an appreciable fraction of the total specimen thickness, the stresses and strains produced may become so large as to cause specimen behavior to differ considerably from that of a linear elastic solid, assumed in the theoretical analysis. Tests were made on several specimens of different materials in an attempt to determine the limit of indentation for which the analysis would still apply, as indicated by a significant change in the computed shear modulus from that for lesser indentations, all other conditions being the same.

Table II. Indentation Test Data for Solthane 113 Specimens

For all test conditions:

Specimen dimensions approximately:  $0 \times 1.25 \text{ in.}$

Specimen thickness =  $h = 0.376 \text{ in.}$

Poisson's ratio =  $\nu = 0.5$  assumed

Temperature  $77^\circ\text{F}$

Readings taken after 2 min. relaxation at constant indentation

Specimen surfaces dusted with talcum powder

Indicator Radius, R (in.)	Penetration Rate (in./min)	Indentation Depth, $w_s$ (in.)	$\frac{H-1}{2} \frac{P}{R^2}$ (Note 1)	Load, P (lb)	Computed Shear Modulus, $G$ (ksi)	
0.0625	2.0	0.025	0.68	1.02	191	
		0.048	1.84	2.78	194	
	0.2	0.048	1.84	2.55	184	
		0.02	0.048	1.84	2.56	182
0.0938	2.0	0.025	0.40	1.27	176	
		0.048	1.06	3.66	190	
		0.074	2.01	6.73	190	
0.1250	2.0	0.023	0.22	1.51	220	
		0.046	0.78	4.36	176	
		0.070	1.25	8.15	210	
		0.095	2.01	12.7	200	
		0.118	2.78	18.4	212	
0.1875	2.0	0.023	0.12	1.55	226	
		0.046	0.40	5.66	205	
		0.070	0.73	10.8	206	
		0.092	1.12	17.4	218	
	0.2	0.046	0.46	5.28	164	
		0.056	1.20	16.8	199	
		0.02	0.046	0.40	5.20	180
			0.097	1.22	16.7	195
0.2500	2.0	0.022	0.09	2.06	188	
		0.045	0.25	6.46	208	
		0.071	0.51	13.7	214	
	0.2	0.048	1.84	2.55	184	
		0.02	0.048	1.84	2.56	182
Mean Value					197	
Standard Deviation					16	
Note 1 - Dimensionless load values from curves, Figure 3.						
Note 2 - Average reading from 2 Runs.						

Table III. Indentation Test Data for Surface Condition Study

For all test runs:

Indenter radius = 0.125 in.

Penetration rate = 2.0 in./min

Temperature 78°F

Load readings taken after 2 min relaxation at constant indentation

Test Specimen Information	Surface Condition (Note 1)	Indentation Depth, $w_0$ (in.)	Load, P (Note 2) (lb)	Computed Shear Modulus $\mu$ (psi)
Hysol 8705 Thickness = $h = 0.504''$ $h/R = 4.0$ $\nu = 0.46$	Dry	0.097	12.8	227
	Soapy	0.106	13.3	209
Solithane 113 Thickness = $h = 0.376''$ $h/R = 3.0$ $\nu = 0.5$	Dry	0.088	11.2	203
	Soapy	0.106	12.2	165

Note 1 - Dry = clean and dry, without talcum powder; soapy = coated with wet soap solution.

Note 2 - Average of 3 runs for each condition.

A definite limit applicable to all specimens was not found, nor was one expected. Any limit would depend on the combined effects of several variables, such as indenter radius and material properties as well as dimensions, and would likely be different for every test situation. The data were nevertheless helpful, in that they indicated no significant deviations for penetrations up to one-third the specimen thickness for any of the specimens tested. Results of deeper penetrations were inconclusive, but in the case of a Solithane 113 specimen did tend to produce higher computed values of shear modulus. Deeper penetrations caused specimens to curl at the edges and to assume a cupped shape, which could be a significant deviation from the geometry of the analysis. In general, then, the maximum allowable penetration depth will be taken as one-third the specimen thickness, unless additional data indicate otherwise.

Following completion of all the previously mentioned tests, the Hysol and Solithane specimens were subjected to a series of tests to evaluate the effects of lateral dimensions, particularly with regard to finding the minimum size required to effectively simulate the infinite extent sheet assumed in the analysis. Here again, no exact limit can readily be defined for the general case because of the interaction of a number of variables.

The procedure consisted of repeating the same test a number of times, trimming the specimen to a smaller size for each run. Data from the particular specimens tested indicate no significant variations in computed shear modulus so long as the specimen length and width are at least 1.5 times the thickness and 6 times the indenter radius. While this may vary for other materials and conditions, there does not appear to be any problem for the types of specimens and conditions for which this test device was designed.

## 2. Viscoelastic Materials Tests

At this time work has only just begun into the study of viscoelastic properties with the indentation tester and very little data are available. However, one series of tests has been performed which is of interest and will be summarized in the following paragraphs.

The materials tested were different compositions of butyl acrylate/acrylic acid/Unox 221<sup>®5</sup> copolymers formulated by Dr. A. R. Pitochelli of these Laboratories. Indentation test data are given in Table IV. Note especially the column of values of  $P_0/P_2$ . These figures compare the peak load,  $P_0$ , read immediately upon reaching the stated indentation depth, to the load,  $P_2$ , after two minutes of relaxation at constant indentation. The ratio  $P_0/P_2$  thus is an indication of the degree of relaxation the material undergoes while under constant strain.

The same data listed in Table IV were also plotted as loads versus time on log-log graph paper, as in Figure 5, for example. The results were approximately straight lines. Thus the load data are quite closely described by the simple equation

$$P(t) = P_e + at^{-m} \quad (5)$$

---

<sup>5</sup>Trademark of Union Carbide Corp., New York, N. Y.

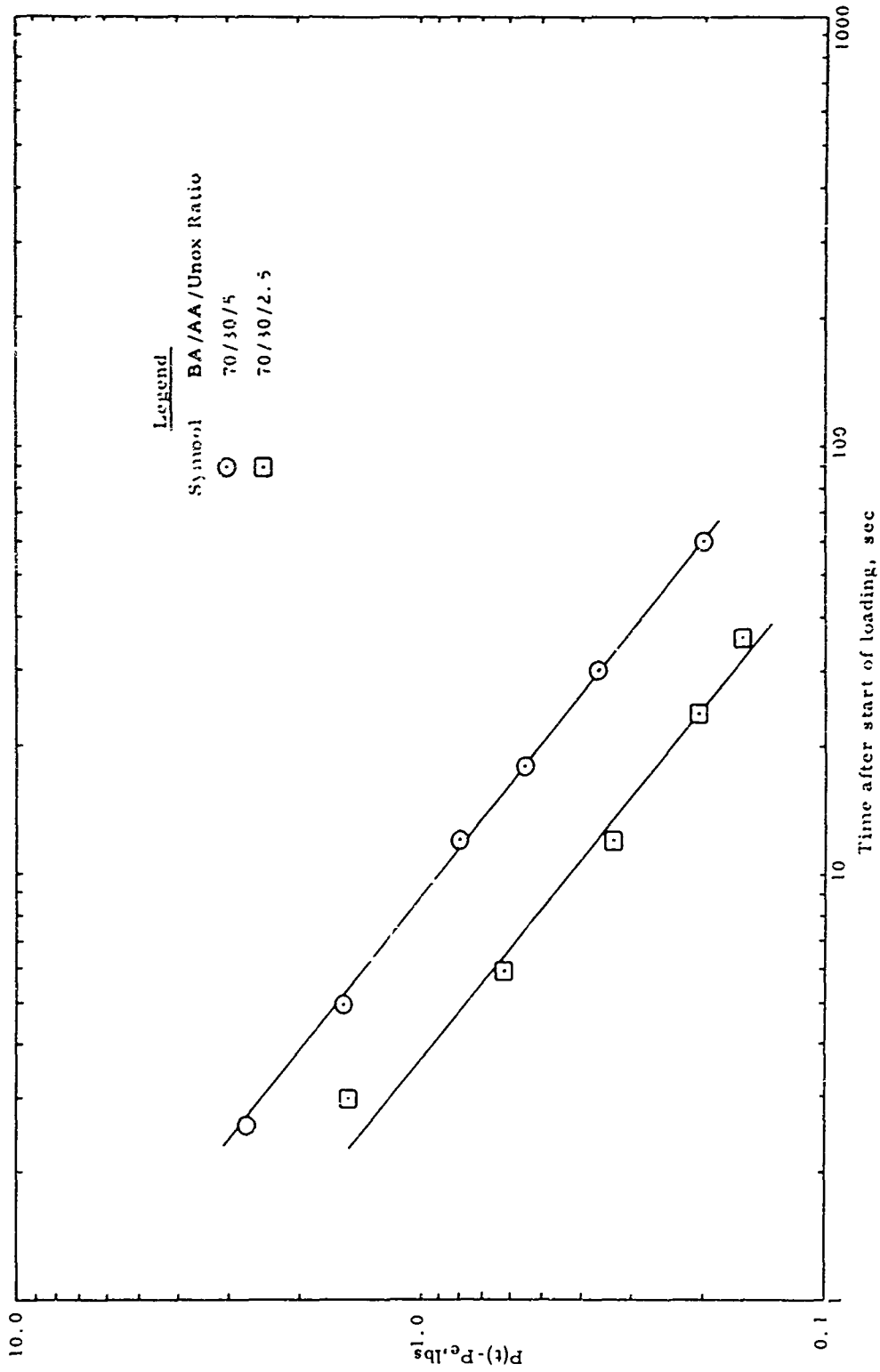


FIGURE 5. VARIATION OF LOAD WITH TIME FOR INDENTATION TESTS OF BA/AA COPOLYMERS

where  $P_e$  is an equilibrium load reached after a relatively long period of time,  $t$  is time, and  $a$  and  $m$  are constants determined for each set of test data to give the best curve fit. If the strain input can be approximately described by a step function [see equation (3) and the related discussion, Section II.2 above], then a plot of load as a function of time may be directly converted to one of shear relaxation modulus,  $\mu(t)$ , by simply changing the scale:

$$\mu(t) = \mu_e + bt^{-m}, \quad (6)$$

where  $\mu_e$  is the equilibrium modulus, and  $b$  is a new constant. Plots of shear moduli,  $\mu(t)$ , versus time obtained in this manner are shown in Figure 6 for several of the copolymers tested.

Composition, Mole Ratios of BA/AA/Unox 221	Shear Modulus, psi	Ratio of Peak Load to Load after 2 min $P_0/P_2$	Remarks (Apply to all Test Runs)
95/5/2.5	30	1.01	Indentor sphere radius: 0.125 in.
95/5/5	35	1.01	Indentation rate: 2.0 in./in./min
90/10/2.5	56	1.01	Indentation depth: Approx. 0.10 in.
90/10/5	59	1.02	Temp: 77°F
85/15/2.5	49	1.08	Rel. humidity: Ambient
85/15/5	75	1.19	Poisson's ratio of 0.5 assumed for all samples
85/15/7.5	116	1.20	
70/30/2.5	40	4.18	Shear modulus computed for load after 2 min relaxation
70/30/5	73	6.25	

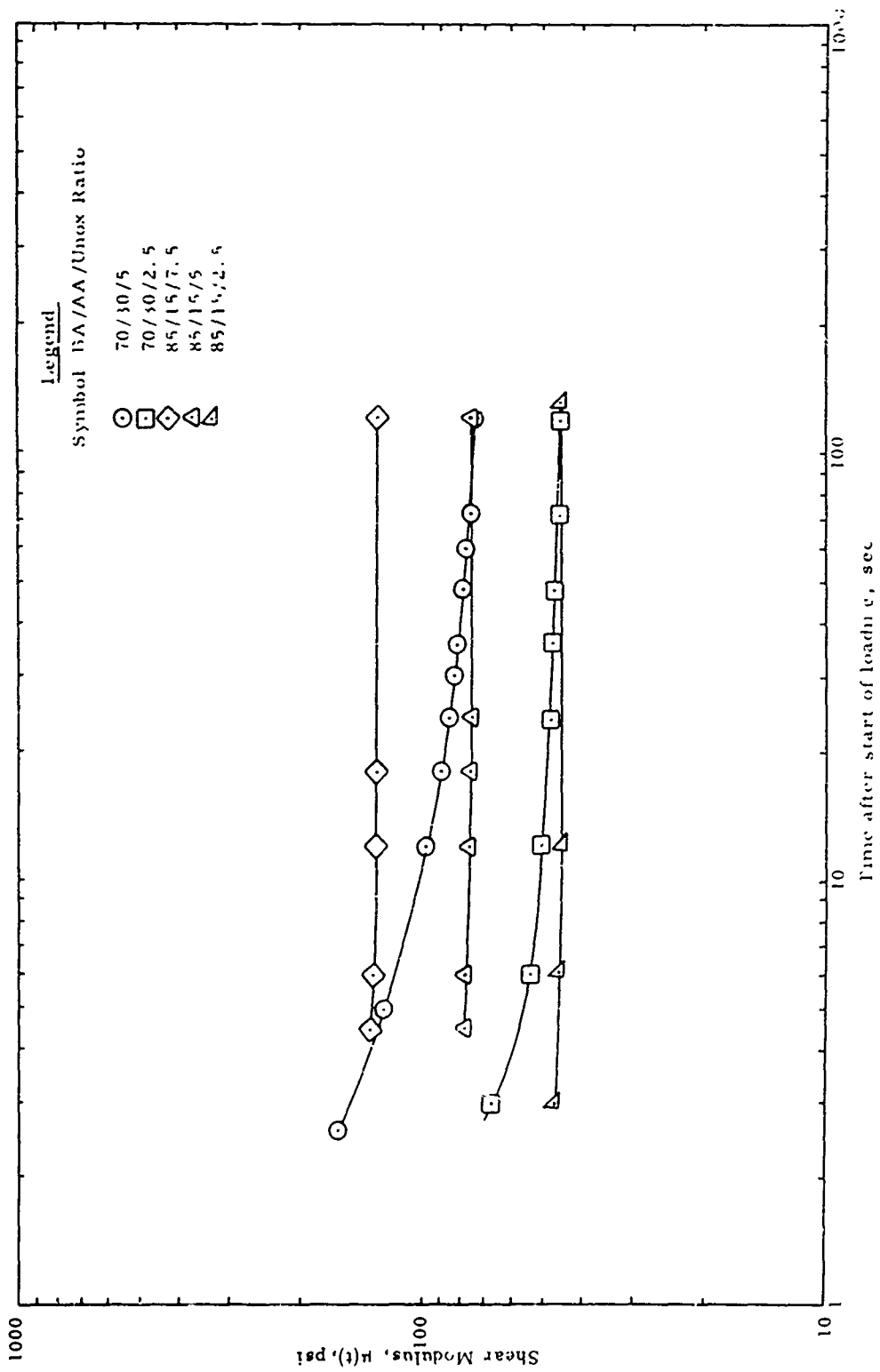


FIGURE 6. SHEAR RELAXATION MODULUS CURVES FOR SEVERAL BA/AA COPOLYMERS, AS OBTAINED FROM INDENTATION TEST DATA

The foregoing indicates that the indentation test may have applications for investigating certain viscoelastic material properties, in addition to its present use in measuring the equilibrium, or elastic, shear moduli. Properties which might be studied include glassy moduli, relaxation times, and the slope of the relaxation curve in the transition region. One must remember, however, that several assumptions and simplifications were made, the validity of which may be open to question. Any attempts to use the method for quantitatively evaluating viscoelastic parameters must await considerable further analysis and experimental confirmation. Nevertheless, the indentation test does have possibilities for immediate use in qualitative studies, such as comparisons of the viscoelastic properties of different materials or of the effects of changing an ingredient in a formulation.

Considering the data of Table IV and Figure 6 in the light of equation (6) leads to the following general statements:

(1) Equilibrium shear moduli,  $\mu_e$ , were found to be directly proportional to the number of crosslinks in the material, determined by the mole fraction of Unox 221. This was an expected result, based upon viscoelastic theory.

(2) The slope of the relaxation curves,  $\mu(t)$ , corresponding to exponent  $m$  in equation (5), appeared independent of crosslinking but increased with increasing acrylic acid content. The slope of relaxation moduli curves can be expected to increase as the test temperature approaches the material glass transition temperature. Glass transition temperature is mainly a function of acrylic acid content for these polymers. Hence, it seems reasonable to conclude that the acrylic acid content, by reason of its influence on glass transition temperatures, has the greatest influence on relaxation characteristics for these copolymers.

(3) There is indicated the possibility of superposing relaxation curves of samples of different composition but having the same degree of crosslinking. For example, the curve for the 85/15/2.5 composition could be shifted to the right in Figure 6 and merged with the curve of the 70/30/2.5 composition to form a single smooth curve. Thus, it would appear that the shape and magnitude of the relaxation curve is a function of crosslinking but its position in time a function of acrylic acid content. This position in time is indicated by the value of the coefficient  $b$  in equation (6).

## Section V. CONCLUSIONS

The indentation test has been shown to be a valid and useful method for determining the shear moduli of relatively low modulus polymers and rubbery materials in the form of thin sheets. Tests conducted over a wide range of conditions of indenter size, specimen size, penetration depth, and penetration rate yielded data which, when reduced according to the theoretical analysis presented, resulted in shear modulus values in close agreement with those obtained by other methods. The indentation test offers the additional advantages of requiring only a small quantity of material and of the need for little, if any, specimen preparation.

Discrepancies noted between indentation test results and moduli obtained by other methods can generally be attributed to experimental variances and tolerances. In particular, a small error in measurement of penetration depth can lead to a much larger error in computing the shear modulus, especially for cases involving a large radius indenter at a small depth. This probably accounts for most of the discrepancies. Another cause could be friction between the specimen surfaces which apparently results in slightly higher load readings and computed moduli. Also, the moduli from other test methods, with which the indentation test results were compared, are themselves subject to the experimental error. All discrepancies noted thus far are considered minor and can be expected to decrease as additional skill and experience are gained.

The indentation test is a potentially useful tool in evaluating viscoelastic properties. Future test efforts will be directed along these lines, with particular emphasis on measurements of relaxation moduli and time-temperature effects. Present plans call for tests with faster loading rates and longer durations, tests at various temperatures, time-temperature superposition studies, and continued evaluation of the areas and limits of application of the test device and theoretical analysis.

## REFERENCES

1. Princeton University, Princeton, N. J., MASTER CURVES FOR SOME AMORPHOUS POLYMERS, M. Takahasi, M. Shen, R. B. Taylor, and A. V. Tobolsky, July 1963, ONR Tech Report RLT-61.
2. Gent, A. N., "On the Relation Between Indentation Hardness and Young's Modulus," Transactions I.R.I., 34, 2, 46-57 (1958).
3. British Standards Institution, 1957, B.S. 903: Part A7.
4. Waters, N.E., "The Indentation of Thin Rubber Sheets by Spherical Indentors," British J. of Appl. Phys., 16, 557-563 (1965).
5. Timoshenko, S. P. and Goodier, J. N., THEORY OF ELASTICITY, Second Edition, New York, McGraw-Hill, 372-382 (1951).
6. Lebedev, N. N. and Ufliand, Ia. S., "Axisymmetric Contact Problem for an Elastic Layer," P.M.M., 22, 3, 320-326 (1958).
7. Parr, C. H., Rohm and Haas Company, "Theory of the Indentation Test for Specimens of Finite Thickness," internal memorandum to A. J. Ignatowski, December 13, 1965.
8. Ignatowski, A. J. and Parr, C. H., "The Development of an Indentation Test for Polymers," ICRPG Mechanical Behavior Working Group, 6th Meeting, Vol. 1, 465-476, October 1967.
9. Lee, E. H. and Radok, J. R. M., "The Contact Problem for Viscoelastic Bodies," J. Appl. Mech., 27, 3, 438-444 (1960).
10. Britton, S. C., "Characterization of Solid Propellants as Structural Materials," Solid Rocket Structural Integrity Abstracts, " Vol. II, 4, 1-71, October 1965.

APPENDIX  
SOLUTION OF THE INDENTATION PROBLEM

1. The Lebedev-Ufliand Solution<sup>6</sup>

Consider the state of elastic equilibrium of a linear elastic layer, infinite in extent but of finite thickness, resting upon a rigid base and undergoing deformation by a rigid punch. The contact surface is a surface of revolution, and the indentation is realized by means of an axial force (Figure 7). It is further assumed that there is no friction between the indenter and layer, or layer and base (although the general method will permit consideration of more involved cases, such as those with adhesion between layer and base).

The boundary conditions imposed by these restrictions are:

$$\tau_{rz} = 0, \quad w = 0 \quad \text{when } z = h, \quad (7)$$

$$\left. \begin{array}{l} \tau_{rz} = 0 \\ w = w_0 - \chi(r) \quad (r < a) \\ \sigma_z = 0 \quad (r > a) \end{array} \right\} \quad \text{when } z = 0, \quad (8)$$

where  $\sigma_z$  and  $\tau_{rz}$  are the normal and tangential stress components, respectively,  $w_0$  is the indentation of the center of the punch, and  $\chi(r)$  is the function describing the punch surface. Cylindrical coordinates  $r, z, \theta$ , are employed.

The solution is facilitated by the use of the Boussinesq-Papkovitch-Neuber displacement functions. The displacements are expressed in the form

$$2 \mu u = - \frac{\partial \Phi_0}{\partial r} - z \frac{\partial \Phi_1}{\partial r}, \quad (9)$$

$$2 \mu w = - \frac{\partial \Phi_0}{\partial z} + (3-4\nu)\Phi_1 - z \frac{\partial \Phi_1}{\partial z}, \quad (10)$$

where  $u$  and  $w$  are radial and axial displacements, respectively,  $\mu$  is the shear modulus,  $\nu$  is Poisson's ratio, and  $\Phi_0$  and  $\Phi_1$  are functions harmonic in the layer  $0 < z < h$ .

<sup>6</sup>Lebedev, N. N. and Ufliand, Ia. S., "Axisymmetric Contact Problem for an Elastic Layer," P.M.M., 22, 3, 320-326 (1958).

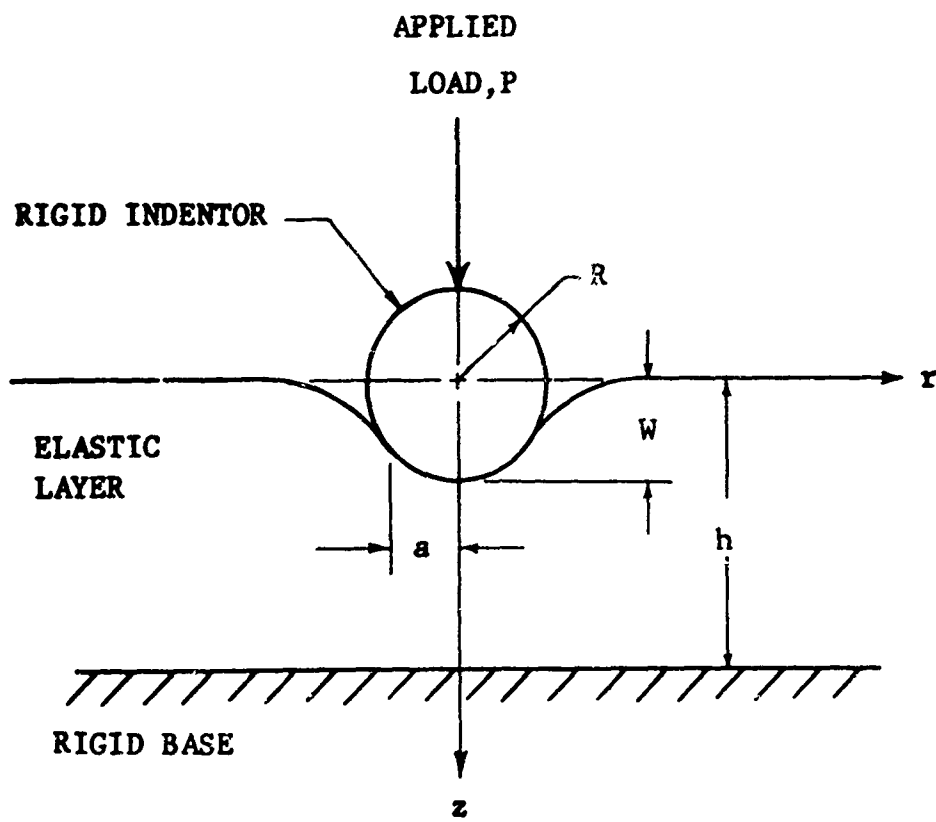


FIGURE 7. GEOMETRY OF INDENTATION PROBLEM

The elastic stresses are expressed in terms of the functions just introduced as

$$\sigma_z = 2(1-\nu) \frac{\partial \Phi_1}{\partial z} - \frac{\partial^2 \Phi_0}{\partial z^2} - z \frac{\partial^2 \Phi_1}{\partial z^2} , \quad (11)$$

and

$$\tau_{rz} = \frac{\partial}{\partial r} \left[ (1-2\nu) \Phi_1 - \frac{\partial \Phi_0}{\partial z} - z \frac{\partial \Phi_1}{\partial z} \right] . \quad (12)$$

Substituting (7) and (8) into the relations (9) through (12) gives the boundary conditions in the following form:

$$\left[ \Phi_1 \right]_{z=h} = 0 \quad . \quad (13)$$

$$\left[ \frac{\partial \Phi_0}{\partial z} + h \frac{\partial \Phi_1}{\partial z} \right]_{z=h} = 0 \quad , \quad (14)$$

$$\left[ (1-2\nu) \Phi_1 - \frac{\partial \Phi_0}{\partial z} \right]_{z=0} = 0 \quad , \quad (15)$$

$$\left[ (3-4\nu) \Phi_1 - \frac{\partial \Phi_0}{\partial z} \right]_{z=0} = 2\mu [w_0 - \chi(r)] , \quad r < a , \quad (16)$$

$$\left[ 2(1-\nu) \frac{\partial \Phi_1}{\partial z} - \frac{\partial^2 \Phi_0}{\partial z^2} \right]_{z=0} = 0 , \quad r > a \quad . \quad (17)$$

The harmonic functions  $\Phi_0$  and  $\Phi_1$  are taken in the form

$$\Phi_1 = \int_0^\infty A(\lambda) \frac{\sinh \lambda (h-z)}{\sinh \lambda h} J_0(\lambda r) d\lambda , \quad (18)$$

and

$$\frac{\partial \Phi_0}{\partial z} = \int_0^\infty \left[ \lambda h A(\lambda) \frac{\cosh \lambda (h-z)}{\sinh \lambda h} + B(\lambda) \frac{\sinh \lambda (h-z)}{\sinh \lambda h} \right] J_0(\lambda r) d\lambda , \quad (19)$$

where  $A(\lambda)$  and  $B(\lambda)$  are functions to be determined and  $J_0(\lambda r)$  is a Bessel function.

If the functions  $\phi_0$  and  $\phi_1$  are selected in this manner, the boundary conditions (13) and (14) will be satisfied for any  $A(\lambda)$  and  $B(\lambda)$ . By substitution into equation (15) we obtain the relation

$$B(\lambda) = [1 - 2\nu - \lambda h \cosh \lambda h] A(\lambda) , \quad (20)$$

while conditions (16) and (17) lead to a system of two integral equations for  $A(\lambda)$ :

$$\int_0^{\infty} A(\lambda) J_0(\lambda r) d\lambda = \frac{F}{1-\nu} [w_0 - \chi(z)] , \quad z < a , \quad (21)$$

$$\int_0^{\infty} \frac{\lambda(\lambda h + \sinh \lambda h \cosh \lambda h)}{\sinh^2 \lambda h} A(\lambda) J_0(\lambda r) d\lambda = 0 , \quad z > a , \quad (22)$$

A solution to equations (21) and (22) is sought in the form

$$A(\lambda) = [1 - g(\lambda)] \int_0^a \phi(t) \cos \lambda t dt \quad (23)$$

where

$$g(\lambda) = \frac{\lambda h + \sinh \lambda h \cosh \lambda h - \sinh^2 \lambda h}{\lambda h + \sinh \lambda h \cosh \lambda h} \quad (24)$$

and  $\phi(t)$  is some unknown function, continuous, together with its derivatives, in the interval  $(0, a)$ .

Manipulations of equation (23) will require the following identities:

$$\int_0^{\infty} J_0(\lambda r) \sin \lambda z \, d\lambda = \begin{cases} 0 & (0 \leq z < r) \\ (r^2 - z^2)^{-\frac{1}{2}} & (z > r) \end{cases} \quad (25)$$

$$\int_0^{\infty} J_0(\lambda r) \cos \lambda z \, d\lambda = \begin{cases} (r^2 - z^2)^{-\frac{1}{2}} & (0 \leq z < r) \\ 0 & (z > r) \end{cases} \quad (26)$$

$$J_0(\lambda r) = \frac{2}{\pi} \int_0^{\pi/2} \cos(\lambda r \sin \theta) \, d\theta \quad (27)$$

Upon integrating the right-hand portion of (23) by parts, substituting the resulting expression for  $A(\lambda)$  into equation (22), and making use of formula (25), we may show that equation (22) is satisfied identically. Details of these steps will not be shown here.

Substitution of  $A(\lambda)$  into equation (21) and making use of the formulas (26) and (27) leads to the relation

$$\begin{aligned} & \int_0^{\infty} \phi(t) (r^2 - t^2)^{-\frac{1}{2}} \, dt - \\ & \frac{2}{\pi} \int_0^{\pi/2} d\theta \int_0^a \phi(t) \, dt \int_0^{\infty} g(\lambda) \cos \lambda t \cos(\lambda r \sin \theta) \, d\lambda \\ & = \frac{\mu}{1-\nu} [w_0 - \chi(r)] \end{aligned} \quad (28)$$

Introducing a new integration variable  $t = r \sin \theta$  into the first integral and manipulating (28) further, there results

$$\int_0^{\pi/2} \left\{ \phi(r \sin \theta) - \frac{1}{\pi} \int_0^a \phi(t) [G(t + r \sin \theta) + G(t - r \sin \theta)] \, dt \right\} d\theta = f(r) \quad (29)$$

where

$$f(r) = \frac{\mu}{1-\nu} [w_0 - \chi(r)] \quad (30)$$

and

$$G(x) = \int_0^x g(\lambda) \cos \lambda x \, d\lambda \quad (31)$$

the Fourier cosine transform of the function  $g(\lambda)$ . Putting

$$F(x) = \phi(x) - \frac{1}{\tau} \int_0^a \phi(t) [G(t+x) + G(t-x)] \, dt \quad (32)$$

then equation (29) will have the form of Schlömilch's integral equation<sup>7</sup>

$$\int_0^{\pi/2} F(r \sin \theta) \, d\theta = f(r) \quad (33)$$

which has the solution

$$F(x) = \frac{2}{\tau} \left[ f(0) + x \int_0^{\pi/2} f'(x \sin \theta) \, d\theta \right] \quad (34)$$

where the prime denotes the derivative. The result of the foregoing is an integral equation for the unknown function  $\phi(t)$ :

$$\begin{aligned} \phi(x) - \frac{1}{\tau} \int_0^a \phi(t) [G(t+x) + G(t-x)] \, dt \\ = \frac{2\mu}{\tau(1-\nu)} \left[ w_0 + x \int_0^{\pi/2} \chi'(x \sin \theta) \, d\theta \right], \quad 0 \leq x \leq a. \quad (35) \end{aligned}$$

<sup>7</sup>Whittaker, E. T. and Watson, G. N., A COURSE OF MODERN ANALYSIS, Fourth Edition, Cambridge University Press, 229 (1958).

If it is possible to find a solution to the integral equation (35) in the form of a function with a continuous derivative, then equations (18), (19), (20), and (23) give a complete solution of the contact problem under consideration.

Many quantities of interest can be expressed immediately in terms of the function  $\phi(t)$ , omitting the intermediate formulas. For example, taking the general expression for stress as given in (11), using the functions defined in (18) and (19), and making the substitutions of (20), (23), and (24), gives the expression for the distribution of normal stresses directly beneath the punch, on the surface  $z = 0$ :

$$[\sigma_z]_{z=0} = \int_r^a \frac{\phi(t) dt}{\sqrt{t^2 - r^2}} - \frac{\phi(a)}{\sqrt{a^2 - r^2}}, \quad r < a. \quad (36)$$

Integrating (36) over the area of the circle of radius  $a$ , we find

$$P = 2\pi \int_0^a \phi(t) dt \quad (37)$$

in which  $P$  is the total applied force to the punch.

## 2. Application to the Indentation Test

In an indentation test the only easily measured quantities are the indenter dimensions, the maximum penetration depth  $w_0$ , and the applied load  $P$ . Therefore, to be of any use to the experimenter the Lebedev-Ufliand solution must be in a form which permits direct calculation of the shear modulus from these measurable quantities.

The following analysis is based upon the use of a spherical indenter, which has the contour

$$\chi(r) = R - \sqrt{R^2 - r^2}, \quad (38)$$

where  $R$  is the radius of the sphere. Then equation (35) takes the form

$$\begin{aligned} \phi(x) &= \frac{1}{\tau} \int_0^a \phi(t) [G(t+x) + G(t-x)] dt \\ &= \frac{2\mu w_0}{\tau(1-\nu)} \left[ 1 + \frac{x}{2w_0} \ln \left( \frac{R-x}{R+x} \right) \right] \end{aligned} \quad (39)$$

At this point it becomes convenient to introduce the dimensionless quantities:

$$\frac{x}{a} = \xi, \quad \frac{t}{a} = \tau, \quad G(x) = K(\xi),$$

$$\phi(x) = \frac{2\mu w_0}{\tau(1-\nu)} \omega(\xi),$$

$$\rho = \frac{a}{R}, \quad \text{and } p = \frac{a}{h}.$$

Equation (39) now becomes

$$\begin{aligned} \omega(\xi) &= \frac{1}{\tau} \int_0^1 \omega(\tau) [K(\tau+\xi) + K(\tau-\xi)] d\tau \\ &= 1 + \frac{\rho\xi}{2 \left( \frac{w_0}{R} \right)} \ln \left( \frac{1-\rho\xi}{1+\rho\xi} \right) \end{aligned} \quad (40)$$

where, from equation (31)

$$K(u) = p \int_0^{\infty} \left[ 1 - \frac{\sinh^2 \alpha}{\alpha + \sinh \alpha \cosh \alpha} \right] \cos \alpha pu d\alpha \quad (41)$$

where, for convenience,  $\alpha = \lambda h$ . Note that the range of  $\xi$ ,  $\tau$ , and  $\rho$  is from 0 to 1.

The formula for the applied force, (37), assumes the following form in dimensionless variables:

$$\frac{(1-\nu)P}{\mu R^2} = 4\rho \frac{w_0}{R} \int_0^1 \omega(\xi) d\xi. \quad (42)$$

From the condition of continuity of stresses at radius  $a$ , it can be deduced that

$$\phi(a) = 0 = \omega(1) \quad (43)$$

Applying this to equation (40) yields the expression

$$\frac{w_0}{R} = \frac{\frac{\rho}{2} \ln \left( \frac{1+\rho}{1-\rho} \right)}{1 + \frac{1}{\pi} \int_0^1 \omega(\tau) [K(\tau+1) + K(\tau-1)] d\tau} \quad (44)$$

Substitution of (44) into (40) gives

$$\begin{aligned} \omega'(\xi) = 1 - \xi \frac{\ln \left( \frac{1+\rho\xi}{1-\rho\xi} \right)}{\ln \left( \frac{1+\rho}{1-\rho} \right)} + \frac{1}{\pi} \int_0^1 \omega(\tau) \left\{ [K(\tau+\xi) + K(\tau-\xi)] \right. \\ \left. - \xi \frac{\ln \left( \frac{1+\rho\xi}{1-\rho\xi} \right)}{\ln \left( \frac{1+\rho}{1-\rho} \right)} [K(\tau+1) + K(\tau-1)] \right\} d\tau, \end{aligned} \quad (45)$$

which is a Fredholm integral equation of the second kind.

The problem now becomes one of solving the integral equation (45) for the function  $\omega(\xi)$ . Once this has been done, the dimensionless load,  $(1-\nu)P/\mu R^2$ , and dimensionless deflection,  $w_0/R$ , can be obtained. In the general case it is necessary to use numerical methods.

### 3. Numerical Solution of Equations

Solution of equation (45) involves first finding values for the function  $K(u)$  in the interval  $0 < u < 2$ . The function  $K(u)$ , equation (41), itself involves the integral of an oscillating function over an infinite interval which cannot be evaluated in closed form. Filon's method was found to perform the indicated quadrature adequately by evaluating  $K(u)$  for the finite interval  $0 \leq \alpha \leq 10$  in increments of 0.2. This was programmed as a subroutine. For the solution of

the integral equation (45), a Gauss-Legendre quadrature was used. In this manner (45) may be rewritten

$$\omega(\tau_i) - \frac{1}{2\pi} \sum_{j=1} A_j \omega(\tau_j) [K(\tau_j + \tau_i) + K(\tau_j - \tau_i)] \quad (46)$$

$$- \tau_i \left[ \frac{\ln \left( \frac{1 + \rho \tau_i}{1 - \rho \tau_i} \right)}{\ln \left( \frac{1 + \rho}{1 - \rho} \right)} \right] [K(\tau_j + 1) + K(\tau_j - 1)] = 1 - \tau_i \left[ \frac{\ln \left( \frac{1 + \rho \tau_i}{1 - \rho \tau_i} \right)}{\ln \left( \frac{1 + \rho}{1 - \rho} \right)} \right]$$

where the  $A_j$  are weighting coefficients and the  $\tau_i$  and  $\tau_j$  are roots of the Legendre polynomial of degree  $N$ . The resulting set of equations is solved for values of  $\omega$  at  $\xi = \tau_i$ . These values of  $\omega$  are, in turn, used in evaluating (42) and (44) by Gauss-Legendre quadrature. The results are presented in the body of the report (see Figures 2 and 3) as curves of dimensionless load  $(1-\nu)P/\mu R^2$  versus dimensionless indentation  $w_0/R$  for various values of  $h/R$ , the ratio of indenter radius to slab thickness.

DOCUMENT CONTROL DATA R 2 D		
<i>(Security Classification of DDCs, body of abstract and indexing annotation must be entered when the original report is classified)</i>		
1. ORIGINATING ACTIVITY (Corporate author) Rohm and Haas Company Redstone Research Laboratories Huntsville, Alabama 35807		2a. REPORT SECURITY CLASSIFICATION Unclassified
		2b. GROUP
3. REPORT TITLE DEVELOPMENT OF A BALL INDENTATION TEST FOR SAMPLES OF FINITE THICKNESS		
4. DESCRIPTIVE NOTES (Type of report and inclusive dates)		
5. AUTHOR(S) (Last name, middle initial, first name) William M. Sigmon, Charles H. Parr, Albert J. Ignatowski		
6. REPORT DATE December 1968	7a. TOTAL NO OF PAGES 36	7b. NO OF REFS 10
8a. CONTRACT OR GRANT NO DAAH01-67-C-0655 A. PROJECT NO DAAH01-68-C-0632	9a. ORIGINATOR'S REPORT NUMBER(S) Technical Report S-182	
c.	9b. OTHER REPORT NO(S) (Any other numbers that may be assigned this report)	
d.		
10. DISTRIBUTION STATEMENT Initial distribution of this report has been made in accordance with contractual agreements. Qualified users may obtain from Defense Documentation Center.		
11. SUPPLEMENTARY NOTES		12. SPONSORING MILITARY ACTIVITY U. S. Army Missile Command Redstone Arsenal, Alabama 35809
13. ABSTRACT <p>A spherical indentation test for small quantities of low modulus materials is described and experimentally validated. The data analysis takes into account finite sample thickness. Comparison with the Hertz contact theory is made, and extension to viscoelastic characterization is discussed.</p>		

DD FORM 1473

REPLACES DD FORM 1473, 1 JAN 64, WHICH IS OBSOLETE FOR ARMY USE

14. KEY WORDS	LINK A		LINK B		LINK C	
	ROLE	WT	ROLE	WT	ROLE	WT
Solid Propellant Mechanical Property Testing Shear Modulus Viscoelastic Properties Indentation Test Solithane <sup>®</sup> Rubber Hysol <sup>®</sup> Rubber						

## **DISCLAIMER NOTICE**

**THIS DOCUMENT IS BEST QUALITY PRACTICABLE. THE COPY FURNISHED TO DTIC CONTAINED A SIGNIFICANT NUMBER OF PAGES WHICH DO NOT REPRODUCE LEGIBLY.**